JAST. Vol. 9, No. 2, pp 1-13

JAST
Journal of Aerospace Science and Technology

A Novel System-Level Calibration Method for Gimballed Platform IMU Using Optimal Estimation

H. Darwish Alshaddadi[1], M.R. Arvan and A.R. Vali[2]

An accurate calibration of inertial measurement unit errors is increasingly important as the inertial navigation system requirements become more stringent. Developing calibration methods that use as less as possible of IMU signals has also become a challenge. In the present work, first a mathematical model of a 6-DOF gimballed IMU in space-stabilized mode is presented. It is considered as held stationary in the test location incorporating 15 different error sources, including accelerometers bias, scale factor error, gyros drift, initial alignment error, and IMU case installation error. Using kinematic relations between IMU platform, IMU body, and IMU platform centered inertial reference frame, six differential equations of the only system-level IMU velocity and gimbal angle are derived. Then the extracted model is validated for error-free case using Sim-Mechanics MATLAB SIMULINK tools to evaluate the introduced mathematical model. Simulation results for 24 hours point out the correctness of the developed model in error-free case. The IMU error analysis methodology incorporates 21-state extended Kalman filter and uses only system-level IMU velocity and gimbal angle measurements taken during one and a half hour with 9 platform attitudes test to estimate IMU error sources. Without the need to install IMU at rotating table, different platform attitudes are achieved using consequent rotations of gimbals. IMU error sources estimation is accomplished off-line. This paper describes the design and test results of a new gimballed IMU calibration method without using a rotating table, and error model development methodology formulated to support the design and test of EKF algorithm and two optimal smoothers: forward-backward and RTS. Results obtained from EKF implementation indicate that the technique is comprehensive and accurate, and requires less specialized test equipments. Also, results show that constant states are not smooth-able. Additional measurements are still helpful for refining an estimate of a constant state.

***Keywords**: Gimballed IMU, space-stable IMU, EKF,- RTS, forward-backward.*

1 Introduction

IMU is the heart of the inertial navigation system. Its function is to supply acceleration signals which are or can be resolved into components of the desired coordinate system [1]. IMU conventionally is a platform which contains three accelerometers mounted on a platform. This platform stays stable in a desired coordinate reference frame. In order to isolate this platform from the vehicle maneuvering, it is usually supported by gimbals which allow the housing the full freedom of motion about the platform. For platform isolation three gyros are mounted with the accelerometers on the platform. Any attempt of the platform to rotate will be sensed by one or more of the gyros and correction signals will be sent to the appropriate gimbal servo motor.

The arrangement of the gimbals varies from system to system, typically, the innermost or first gimbal is the stable element containing the gyros and accelerometers. The first or azimuth gimbal is free to rotate about its axis and the platform is often oriented in the vehicle so that the first gimbal axis is vertical. The axis of azimuth

1. Malek-Ashtar University of Technology (MUT),Tehran, Iran
2. hosam.shadadi@gmail.com, arvan@mut.ac.ir, ar.vali@gmail.com

gimbal is mounted on the second or pitch gimbal which is in turn mounted on the third or roll gimbal [2], Figure 1. No matter how the vehicle maneuvers, the pickoff on the innermost gimbal measures azimuth, the pickoff on the middle gimbal measures pitch, and that on the outer gimbal measures roll, which forms the first IMU output set.

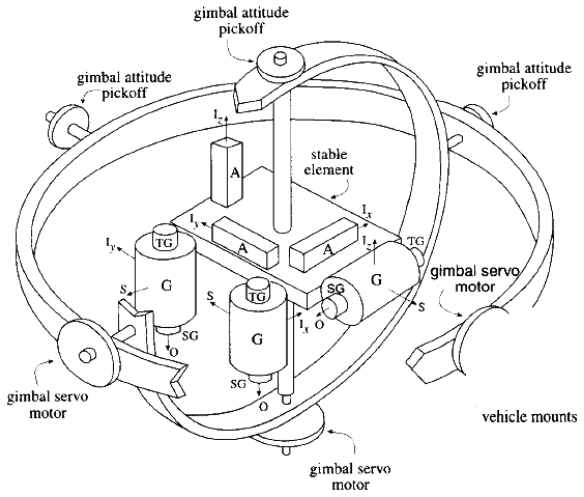

Figure 1. Schematic of a gimballed inertial measurement unit [2]

Accelerometers triad mounted on the platform measure the specific force which is proportional to the difference between the acceleration of the vehicle and the earth gravitational acceleration coordinated in a suitable reference frame. In some IMU types, accelerometers output signals are not available at system-level, where they are integrated internally and corresponding velocity signals are accumulated as the second IMU output set [3].

Figure 2. Real gimballed inertial measurement unit

In Figure 1 the picture of a real gimballed inertial measurement unit with transparent case is shown.

The space-stabilized IMU physically instruments an inertial frame. In this mechanization, the gyros are uncommanded and the accelerometers measure the specific force which is proportional to the difference between the inertial referenced acceleration and the earth gravitational acceleration [1, 2], Figure 3. The commanded platform angular velocity will be ideally equal to the desired level which is zero.

A detailed 2-DOF gimbal inertial stabilized platform model is presented in [10], incorporating all nonlinearities torque such as 2-DOF gimbal inertia disturbances, friction, cable restraint, noise, as well as other disturbances from the outside environment and vehicle body motion. Those are modeled as uncertain linear model.

The accuracy of an inertial navigation system (INS) is affected strongly by its IMU accuracy which contains some deterministic and non-deterministic errors. These deterministic errors should be determined by comparing IMU measurements with known reference information like earth gravitational field and angular velocity; and this procedure is called calibration. Then, by correcting IMU measurements by these estimated errors, INS accuracy should be improved. This process is called compensation. Various kinds of calibration methods have been developed due to the paramount importance of the calibration process for every INS. The most commonly used calibration methods are using precise laboratory instruments,collecting data by orienting the IMU in different attitudes,using adjustment techniques for determining errors, and/or using different de-noising techniques (filtering).

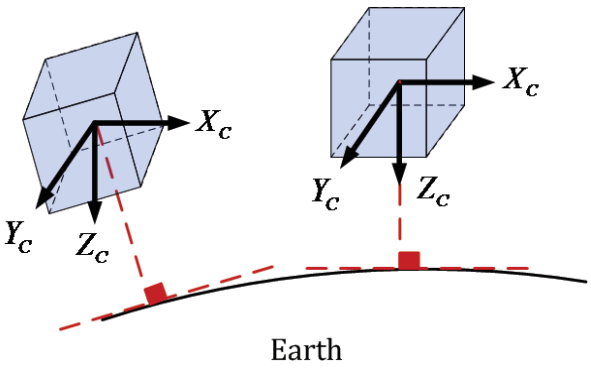

Figure 3. Space-stable inertial measurement unit

A new calibration technique that does not require any additional equipment other than the IMU itself, with no need to special alignment is developed in [4] where the deterministic sensor errors are estimated by recording IMU data for different attitudes. A modification for the traditional six-position calibration technique in [5] enables the calibration process to estimate non-orthogonality errors in addition to accelerometers bias, gyros drift, and scale factors errors. Based on the fact that

in stationary modes, the total magnitude that gyros and accelerometers sense will be the earth rotational rate and the gravity magnitude, respectively, independent of the direction that the individual axes are pointing, a "g-square" calibration method is described in [6]. A novel experimental design to greatly improve the calibration accuracy of the acceleration-insensitive bias and the acceleration-sensitive bias of the dynamically tuned gyroscopes (DTGs) is presented in [7].

In [8] a fast and accurate stationary alignment method for strapdown inertial navigation system (SINS) is proposed. Here a novel azimuth error estimation algorithm was applied. Consequently, the speed and accuracy of the initial alignment of the SINS is enhanced greatly. In [9] an algorithm was proposed to estimate the azimuth misalignment angle and gyro drift rates from the rates of leveling misalignment angles without using the gyro output signals. In [10] for realizing the self-calibration of small gesture platform in the missile before launch, the author analyzed and fixed the accurate error models, designed the circuit of the rotating control and tested it. Depending on the directional conditions and stabilization of the platform, the platform carried out automatism rotation, lock and test. Combining the error models, the error coefficients were separated from the output of the gyroscopes and accelerometers. In [11] an integral scheme of 16 position error calibration and autonomous alignment for three axis platform is given. It may calibrate 42 errors on the whole, including the determining orientation, and will take about 70 minutes.

Since IMU measurements are noise contaminated data, the need to use mathematical filtering techniques is vital. Different stochastic estimation techniques have been introduced to estimate IMU errors, among the entire techniques Kalman filter is considered the most commonly in estimating the values of state variables of a dynamics system which is excited by stochastic disturbances and stochastic measurement noise.

A 53-state Kalman filter is implemented in [3] by using only system-level IMU velocity and gimbal angle measurements taken during a two and a half hour and twelve-platform attitude test to estimate significant error sources of IMU relative to the inertial instrument random disturbances. Fast calibration technique by Kalman filtering with the modified level axis Schuler error loop in which the Schuler factor is introduced in order to be able to change the Schuler period is proposed in [12]. Simulation results show that the proposed calibration technique has led to enhanced accuracy in the instrument errors estimation while reducing the calibration test time. A simple method to calibrate the accelerometer cluster of an IMU is proposed in [13]. By rotating the IMU into different unknown orientations and assuming that the IMU is stationary in each location as the sensor noise is white Gaussian distribution, the system calibration is done using the maximum likelihood estimation method.

In this paper a novel approach is introduced for calibration of gimballed platform IMU by using optimal estimation algorithms. These algorithms use the system-level IMU velocity and gimbal angle measurements during one and a half hour with 9 different platform attitudes of IMU. 15 different error sources, including accelerometers bias, scale factor error, gyros drift, initial alignment error, and IMU case installation error are estimated by this calibration method.

Chapter II presents a mathematical model of 6-DOF gimballed IMU which is derived considering 15 error parameters and using kinematic relations between IMU platform, IMU body, and inertial reference frames. Then, the obtained model is validated for error-free case using SimMechanics MATLAB SIMULINK tools. Next, the new gimballed IMU error parameters calibration methodology is presented in chapter III where only system-level IMU velocity and gimbal angles measurements taken during a one and a half hour and nine platform attitudes test are incorporated to estimate significant IMU error sources. Chapter IV formulates the implemented EKF and both forward-backward and RTS smoothers. Simulation results are given in chapter V.

2 Gimballed IMU Mathematical Model

Before starting the modeling process, a useful reference frame named auxiliary inertial frame (X_i, Y_i, Z_i), should be defined to be used later as a reference frame for all vectors representations. The auxiliary inertial frame is simply an inertial frame where in which its origin and axes orientation coincide with those of the navigation frame (N,E,D) at navigation starting time, Figure 4.

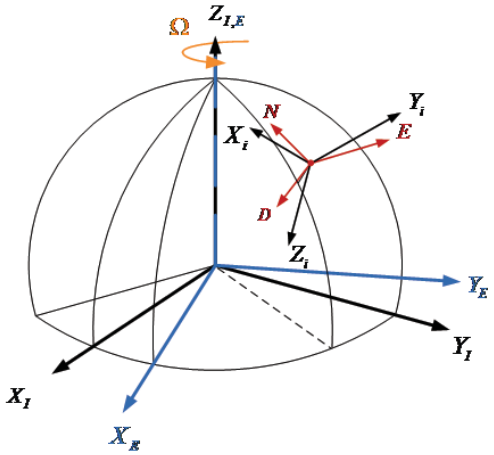

Figure 4. Reference frames

A. Gimbals angles pickoffs modeling

The angular velocity vector of the platform frame relative to the inertial frame coordinated in platform frame

coordinates is given as:

$$ {}^{p}\vec{\omega}_{p/i} = {}^{p}\vec{\omega}_{p/g} + {}^{p}_{g}C\ {}^{g}\vec{\omega}_{g/i} \tag{1} $$

where

${}^{g}\vec{\omega}_{g/i}$ is the angular velocity vector of the gyro frame relative to the inertial frame coordinatized in gyro frame coordinates,

${}^{p}\vec{\omega}_{p/g}$ is the angular velocity vector of the platform frame relative to the gyro frame coordinatized in platform frame coordinates, and because gyros are fixed to IMU platform, it equals to zero,

$\vec{\omega}_{g/i}$ is composed of two basic vectors [14]. The first represents the angular velocity at which the gyros are commanded to process relative to auxiliary inertial frame. $\vec{C}_{g}$ The second represents gyro frame angular velocity relative to auxiliary inertial frame due to all gyro imperfections and is commonly referred to as gyro drift. $\vec{D}_{g}$ Our case is space-stabilized IMU, that is, the gyros are uncommanded and $\vec{C}_{g} = \vec{0}$. Subsequently, the, and equation (1) becomes

$$ {}^{p}\vec{\omega}_{p/i} = {}^{p}_{g}C\ {}^{g}\vec{D}_{g} \tag{2} $$

On the other hand, using consequent rotations of yaw, pitch, and roll gimbals, ${}^{p}\vec{\omega}_{p/i}$ can be written as follows

$$ {}^{p}\vec{\omega}_{p/i} = {}^{p}\vec{\omega}_{p/PG} + {}^{p}\vec{\omega}_{PG/RG} + {}^{p}\vec{\omega}_{RG/B} + {}^{p}\vec{\omega}_{B/i} \tag{3} $$

Where B, RG and PG refer to IMU body, roll, and pitch gimbals, respectively.

Assuming that the IMU is rigidly mounted to on a static test fixture, IMU case angular velocity is simply that of the rotating earth and equation (3) can be written in the following form

$$ {}^{p}\vec{\omega}_{p/i} = {}^{p}\vec{\omega}_{p/PG} + {}^{p}_{PG}C \left\{ {}^{PG}\vec{\omega}_{PG/RG} + {}^{PG}_{RG}C \left({}^{RG}\vec{\omega}_{RG/B} + {}^{RG}_{B}C\ {}^{B}_{n}C\ {}^{n}\vec{\omega}_{n/i} \right) \right\} \tag{4} $$

Using equations (2) and (4), time rates of change of IMU gimbals pickoffs angles are given by

$$ \begin{aligned} \dot{\theta}_{x} &= \frac{C_{\theta_z} D_{gx} - S_{\theta_z} D_{gy}}{C_{\theta_y}} - \Omega S_{L} \eta_{y} \\ &+ \frac{S_{\theta_y}}{C_{\theta_y}} \{ \Omega C_{L} [\eta_{z} S_{\theta_x} + \eta_{y} C_{\theta_x}] + \\ &+ \Omega S_{L} [\eta_{x} S_{\theta_x} - C_{\theta_x}] \} - \Omega C_{L} \end{aligned} \tag{5} $$

$$ \begin{aligned} \dot{\theta}_{y} &= \Omega C_{L} \left\{ \eta_{z} C_{\theta_x} - \eta_{y} S_{\theta_x} \right\} + \Omega S_{L} \left\{ \eta_{x} C_{\theta_x} + S_{\theta_x} \right\} \\ &+ S_{\theta_z} D_{gx} + C_{\theta_z} D_{gy} \end{aligned} \tag{6} $$

$$ \begin{aligned} \dot{\theta}_{z} &= D_{gz} - S_{\theta_y} \left\{ \Omega C_{L} + \Omega S_{L} \eta_{y} + \dot{\theta}_{x} \right\} \\ &- C_{\theta_y} \{ \Omega C_{L} \{ \eta_{z} S_{\theta_x} + \eta_{y} C_{\theta_x} \} \\ &+ \Omega S_{L} \{ \eta_{x} S_{\theta_x} - C_{\theta_x} \} \} \end{aligned} \tag{7} $$

Where

D_{g}: Gyros drift vector
η : IMU case installation errors
Ω : Earth angular velocity
L : Geographic latitude

Gimbals pickoffs angles θ_{x}, θ_{y}, and θ_{z} can be found by solving equations (5), (6), and (7).

B. IMU velocity modeling

The specific force coordinatized in the navigation frame is given by

$$ {}^{n}\vec{f}_{s} = \begin{bmatrix} 0 & 0 & -g \end{bmatrix}^{T} \tag{8} $$

The time derivative of imperfect IMU velocity vector coordinatized in the accelerometer frame is given by

$$ {}^{a}\dot{\vec{V}} = K_{a}\ {}^{a}\vec{f}_{s} + {}^{a}\vec{B}_{a} \tag{9} $$

Where

B_{a} is aaccelerometers bias vector,.

K_{a} is 3x3 diagonal matrix of the actual accelerometers scale factors which differ from $\vec{K}$ the nominal accelerometers scale factor vector by $\overrightarrow{dK}$; that is the accelerometers scale factor error vector.

$$ K_{a} = \begin{bmatrix} K_{x} + dK_{x} & 0 & 0 \\ 0 & K_{y} + dK_{y} & 0 \\ 0 & 0 & K_{z} + dK_{z} \end{bmatrix} \tag{10} $$

So, the derivative of imperfect IMU velocity vector coordinatized in the accelerometer frame becomes

$$ {}^{a}\vec{V} = K_a \, {}^{a}_{p}C \, {}^{p}_{PG}C \, {}^{PG}_{RG}C \, {}^{RG}_{B}C \, {}^{B}_{n}C \, {}^{n}\vec{f}_s + {}^{a}\vec{B}_a \quad (11) $$

Using initial alignment error matrix to write equation (11) in the auxiliary inertial frame gives

$$ {}^{i}\dot{\vec{V}} = {}^{i}_{p}C \, {}^{p}_{a}C \, {}^{a}\dot{\vec{V}} $$
$$ = {}^{i}_{p}C \, {}^{p}_{a}C \left(K_a \, {}^{a}_{p}C \, {}^{p}_{PG}C \, {}^{PG}_{RG}C \, {}^{RG}_{B}C \, {}^{B}_{n}C \, {}^{n}\vec{f}_s + {}^{a}\vec{B}_a \right) \quad (12) $$

Expanding and simplifying equation (12), time derivative components of imperfect IMU velocity vector coordinatized in the auxiliary inertial frame are given by

$$ \dot{V}_x = s_1 + -\zeta_z s_2 + \zeta_y s_3 \quad (13) $$

$$ \dot{V}_y = \zeta_z s_1 + s_2 + -\zeta_x s_3 \quad (14) $$

$$ \dot{V}_z = -\zeta_y s_1 + \zeta_x s_2 + s_3 \quad (15) $$

where

$$ s_1 = K_{ax} a_1 + B_{ax} $$
$$ s_2 = K_{ay} a_2 + B_{ay} $$
$$ s_3 = K_{az} a_3 + B_{az} $$
$$ a = -g \left(S_{\theta_z} S_{\theta_x} - C_{\theta_z} S_{\theta_y} C_{\theta_x} \right) $$
$$ a = -g \left(C_{\theta_z} S_{\theta_x} + S_{\theta_z} S_{\theta_y} C_{\theta_x} \right) $$
$$ a = -g C_{\theta} \, C_{\theta} $$

ζ Initial alignment errors

IMU velocity components: V_x, V_y, and V_z, can be found by solving equations(13), (14), and (15).

C. Gimballed IMU SimMechanics model

Different validation methods can be classified into three groups: validation directly with the original system outputs, comparisons with already provided outputs by other scholars and developing another model using a completely different method which may not be applicable on some systems.

Dealing with such systems is always difficult due to the lack of resources, but we are lucky because our system can be modeled in another way based on kinematic relations, using SimMechanics library in MATLAB SIMULINK. Hence, a perfect (error-free) IMU model can be easily created.

Figure 5 represents the developed model in MATLAB SIMULINK using SimMechanics library blocks, and as we can see the model can be divided into five subsystems as following:

- Earth frame: this subsystem simulates the earth movement relative to earth centered inertial frame *I-frame*. In order to do this a spherical body with a radii equals to earth's one is defined; earth block, and earth reference frame CS1 is also defined the rotation rate of which is achieved by Rz-revolute block.
- Gimbals: this subsystem is composed of gimbal joint which simulates IMU gimbals and three joint sensors: Rx, Ry, and Rz to measure gimbals rotation angles.
- Platform frame: this subsystem defines platform block which is a body located on the earth surface and connects it to gimbal joint, then adds a body velocity sensor to measure platform linear velocity vector.
- Auxiliary inertial frame: at navigation start time, an auxiliary inertial frame CS1 is defined. To do this a body block is added and connected to *I-frame* using weld joint.
- Gravity vector components: SimMechanics software considers all forces, gravitational and specific ones, that act on the bodies; therefore, the comparison with our mathematical model will be meaningless, unless the gravitational force is excluded. This work is done in the fifth subsystem where time-variant gravity vector components are integrated to be subtracted later from body velocity sensor output.

3 IMU CALIBRATION METHODOLOGY

Since static IMU hardware error sources can be compensated in the operational flight computer program, it is desirable to estimate each significant IMU error source to an accuracy, such that the navigational accuracy achievable with the IMU, that would be limited only by non-compensable random disturbances.

Dealing with the IMU as a black box dictates that only system-level outputs are available and any calibration technique should be able to estimate desired IMU errors using only these available outputs, namely IMU gimbals pickoffs angles and IMU velocities. In other words, "No disassembly" constraint must be respected in developing our calibration technique.

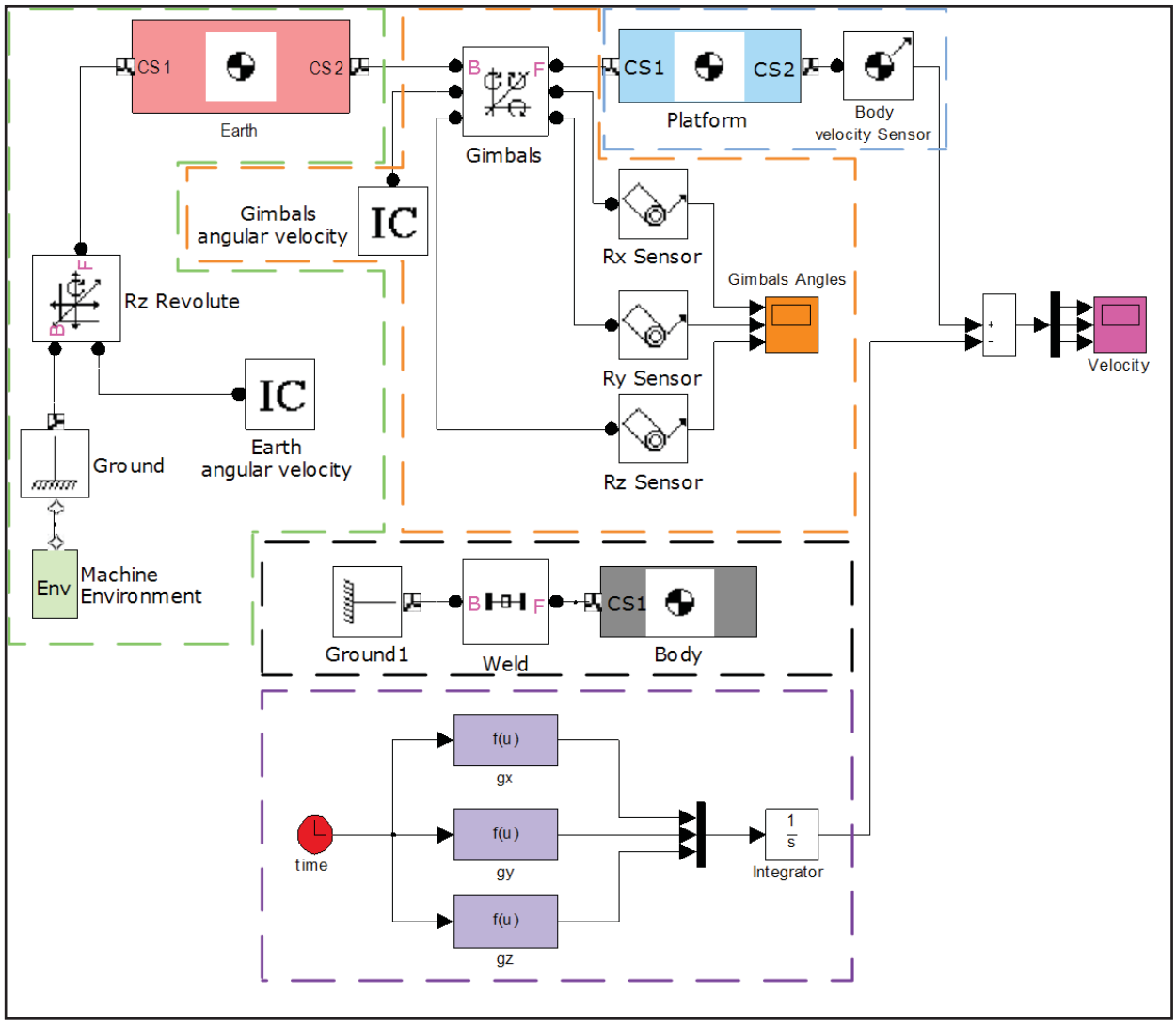

Figure 5. IMU model using SimMechanics tools

Although, any navigation laboratory dealing with gimballed INS calibration is equipped with specialized equipments, we prefer to reduce calibration equipments as much as possible for both decreasing external error sources and enhancing the cost-effectiveness. In addition to the laboratory computer that leads the calibration process, only a precise tilting table used to align IMU case to the navigation frame should be sufficient to conduct our calibration process.

Given that the IMU case is aligned to the navigation frame, different relative platform-to-navigation frame angular orientations can be obtained by gimbal rotations, thus obviating any need to rotate the IMU case. These angular orientations are required for separation of the IMU error sources.

The preceding derivations of IMU output in the previous section have resulted in a set of six general simultaneous equations relating the six-system-level IMU measurable quantities to 15 error sources. Since a set of six specific simultaneous stochastic differential equations cannot be solved for 15 unknowns, a means functionally separating the error quantities had to be formulated. In view of the stochastic nature of the equations and IMU measurement noise, stochastic estimation of the error quantities would be the best solution possible.

The conceptual approach to error source separation is to generate multiple sets of specific simultaneous differential equations from the basic set of six general ones. By generating enough multiple sets of specific equations such that the total number of equations is equal to

the number of unknowns, accurate stochastic estimation of IMU error sources should be possible. The generation of the multiple sets of specific equations is accomplished by angularly orientating the platform at various attitudes relative to the earth rate and gravity vectors by a specific set of gimbal rotations. This approach follows directly from the observation that the measurable IMU outputs are functions of both the IMU error sources and the components of earth rate and gravity vectors in the platform as well as inertial reference frames.

An off-line IMU calibration approach greatly facilitates the development of data analysis computer program since it can be written in a higher order language, and is suitable for in lab calibration techniques.

Finally, total calibration time of few hours or less is recommended to allow aided-inertial navigation software tests to be conducted on the same days as the calibration tests, and to preserve IMU work hours since they are limited.

Although many optimal stochastic estimation techniques are available, the Kalman filter algorithm is considered to be the most applicable approach.

4 OPTIMAL ESTIMATION AND SMOOTHERS

A. EKF ALGORITHM

To write the system model in state space form we should first define the state vector $\underline{x}$, since we want to estimate IMU error parameters included in the derived set of differential equations, and the measurements are only IMU gimbals pickoffs angles and IMU velocities. Therefore, the only choice we have is a (21×1) vector as the following

$$\underline{x} = \begin{bmatrix} \theta_{x,y,z} \\ V_{x,y,z} \\ B_{ax,ay,az} \\ D_{gx,gy,gz} \\ \eta_{x,y,z} \\ dK_{x,y,z} \\ \zeta_{x,y,z} \end{bmatrix} \tag{16}$$

Therefore, system dynamics model can be written as follows:

$$\underline{\dot{x}} = \underline{l}\left(\underline{x}, \Omega, L, g\right) \tag{17}$$

Where

$\underline{l}$ is (21×1) vector and the last 15 components are zeros, since x_7 to x_{21} are constants.

To keep the implementation simple, the continuous-time dynamics equations (17) are discretized using a simple Euler integration scheme to give.

$$\begin{aligned} \underline{x}\left[k+1\right] &= \underline{x}\left[k\right] + T\,\underline{l}\left(\underline{x}, \Omega, L, g\right) \\ &= \underline{f}\left(\underline{x}\left[k\right], \Omega, L, g, T\right) \end{aligned} \tag{18}$$

Completing the system dynamics model by adding process noise we get the following

$$\underline{x}\left[k+1\right] = \underline{f}\left(\underline{x}\left[k\right], \Omega, L, g, T\right) + B\underline{w}\left[k\right] \tag{19}$$

Where

T is sampling time,.

$\underline{f}$ is a resultant (21×1) nonlinear vector of Euler integration,.

$\underline{w} \sim N(0,Q)$ is a (6×1) Gaussian, zero-mean, uncorrelated, white noise,.

and B is (21×6) noise distribution matrix.

The measurements model is discrete and is given by

$$\underline{y}\left[k\right] = H\,\underline{x}\left[k\right] + \underline{v}\left[k\right] \tag{20}$$

Where

$\underline{v} \sim N(0,R)$ is a (6×1) Gaussian, zero-mean, uncorrelated, white noise,.

and H is (6×21) measurement distribution matrix.

Linearization process should take place only on in the system dynamics model since the measurements are in discrete-time form.

$$A_k\left[i,j\right] = \frac{\partial f_i}{\partial x_j}\left(\underline{\hat{x}}\left[k\right]\right) \tag{21}$$

And the Extended Kalman filter algorithm for our case of study is shown in Figure 6.

Considering IMU error parameter as random constants, the great majority of the nonzero (21×21) system matrix A elements are located in the A matrix rows corresponding to the system-level gimbal angle θ and

velocity V measurement states, since IMU error parameter don't does not contribute to any nonzero A matrix elements.

The (21×6) noise distribution matrix B is illustrated in equation(22). This matrix contains six nonzero elements that which are located in the rows corresponding to the gimbal angle θ and velocity V measurements states.

$$B = \begin{bmatrix} I_6 \\ 0_{15\times 6} \end{bmatrix} \tag{22}$$

Where

I_6 is a (6×6) identity matrix,.

and $O_{15\times 6}$ is a (15×6) zeros matrix.

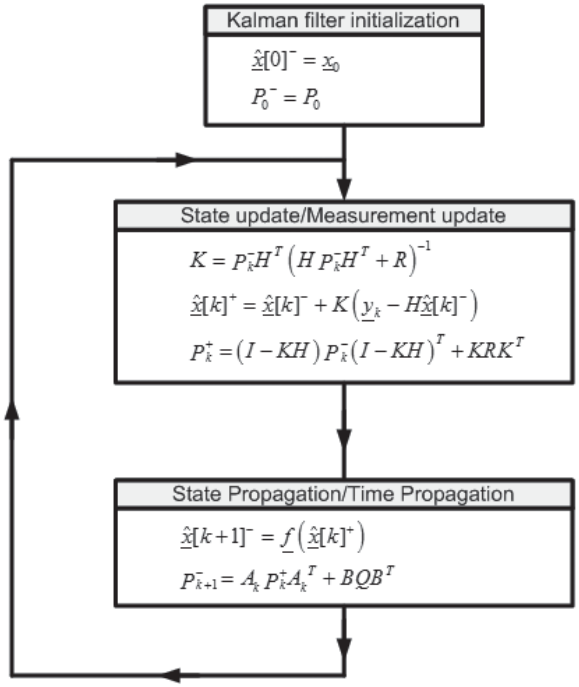

Figure 6. EKF block diagram

The disturbance vector $\underline{w}$ is (6×1) input vector whose elements are zero-mean, white noise processes. These white noise processes are assumed to be uncorrelated with each other resulting in the (6×6) system noise diagonal matrix Q.

$$Q = \begin{bmatrix} \sigma^2_{w_{\theta_x}} & 0 & 0 & 0 & 0 & 0 \\ 0 & \sigma^2_{w_{\theta y}} & 0 & 0 & 0 & 0 \\ 0 & 0 & \sigma^2_{w_{\theta_z}} & 0 & 0 & 0 \\ 0 & 0 & 0 & \sigma^2_{w_{V_x}} & 0 & 0 \\ 0 & 0 & 0 & 0 & \sigma^2_{w_{V_y}} & 0 \\ 0 & 0 & 0 & 0 & 0 & \sigma^2_{w_{V_z}} \end{bmatrix} \text{ Disp} \tag{23}$$

Where

$\sigma_{w_{\theta_x}}$ is θ_x system noise standard deviation.

The (6×21) measurement matrix H contains six nonzero elements of unity magnitude in the columns corresponding to the rows of the gimbal angle θ and velocity V measurement states.

$$H=[I_6 \quad O_{6\times 15}] \tag{24}$$

The measurement noise vector v is a (6×1) vector whose elements are zero-mean, white noise processes. These white noise processes are assumed to be uncorrelated with each other resulting in the (6×6) measurement noise diagonal matrix R.

$$R = \begin{bmatrix} \sigma^2_{V_{\theta_x}} & 0 & 0 & 0 & 0 & 0 \\ 0 & \sigma^2_{V_{\theta y}} & 0 & 0 & 0 & 0 \\ 0 & 0 & \sigma^2_{V_{\theta_z}} & 0 & 0 & 0 \\ 0 & 0 & 0 & \sigma^2_{V_{V_x}} & 0 & 0 \\ 0 & 0 & 0 & 0 & \sigma^2_{V_{V_y}} & 0 \\ 0 & 0 & 0 & 0 & 0 & \sigma^2_{V_{V_z}} \end{bmatrix} \tag{25}$$

Where

$\sigma_{v_{\theta x}}$ is θ_x measurement noise standard deviation.

The (21×21) covariance matrix P is initially a diagonal matrix composed of the IMU error source variances. A partial covariance matrix re-initialization is required each time the platform frame is re-oriented since the variances of the velocity and gimbal angle measurement states having have increased during testing at a given platform attitude and must be reset to zero.

B. Forward-Backward smoothing

To estimate the state $\underline{x}_m$ based on measurements from k=1 to k=N, where N >m, forward-backward approach to smoothing obtains two estimates of $\underline{x}_m$. The first estimate, $\hat{\underline{x}}_{m_f}$, is based on the standard Kalman filter that operates from k=1 to k=m. The second estimate, $\hat{\underline{x}}_{m_b}$, is based on Kalman filter that runs backward in time from k=N to k=m. Then the forward-backward approach to smoothing combines the two estimates to form an optimal smoothed estimate $\hat{\underline{x}}_m$.

$$\hat{\underline{x}}_m = K_f \hat{\underline{x}}_{m_f} + K_b \hat{\underline{x}}_{m_b} \tag{26}$$

Where

K_f and K_b are constant matrix coefficients.

Using both forward covariance matrix, P_f, and backward covariance matrix, P_b, that result from Kalman filter implementation, K_f and K_b can be calculated as follows

$$K_f = P_b \left(P_f + P_b\right)^{-1}$$
$$K_b = P_f \left(P_f + P_b\right)^{-1} \quad (27)$$

The inverse of (P_f+P_b) always exists since both covariance matrices are positive definite [15]. The covariance matrix of the forward-backward smoother is given by

$$P = \left(P_f^{-1} + P_b^{-1}\right)^{-1} \quad (28)$$

To run Kalman filter backwardly, the system equation should be written in reverse form

$$\underline{x}\left[k-1\right] = A_{k-1}^{-1}\underline{x}\left[k\right] + A_{k-1}^{-1}B_{k-1}\underline{w}\left[k-1\right]$$
$$\underline{y}\left[k\right] = H_k\,\underline{x}\left[k\right] + \underline{v}\left[k\right] \quad (29)$$

The inverse A_{k-1}^{-1} should always exist if it comes from a real system. And the forward-backward smoothing algorithm for our case of study is shown in Figure 7.

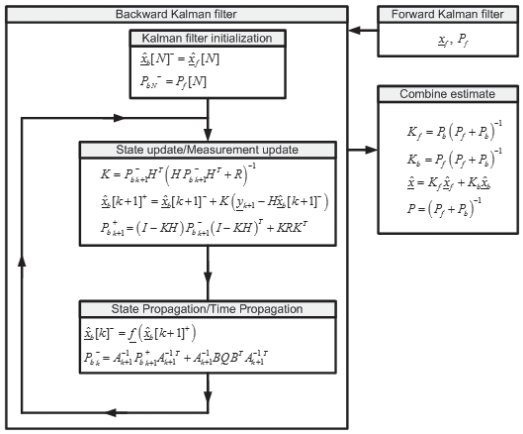

Figure 7. Forward-backward smoother block diagram.

C. RTS smoother

One of the most common smoothers is that was presented by Rauch, Tung, and Striebel, usually called the RTS smoother. RTS smoother is more computationally efficient than forward-backward smoother, because we do not need to directly compute the backward estimate or covariance in order to get the smoothed estimate or covariance [15].

The RTS smoother is implemented by first running Kalman filter forward to the final time N, and then implementing the smoothing equations were presented in Figure 8 backwardly from the final time to the initial time with the following initial conditions.

$$\underline{\hat{x}}\left[N\right]^s = \underline{\hat{x}}\left[N\right]^+$$
$$P_N^s = P_N^+ \quad (30)$$

Where $\underline{\hat{x}}\,[N]^s$ and P_N^s are the smoothed state estimation and error covariance at the N^{th} step.

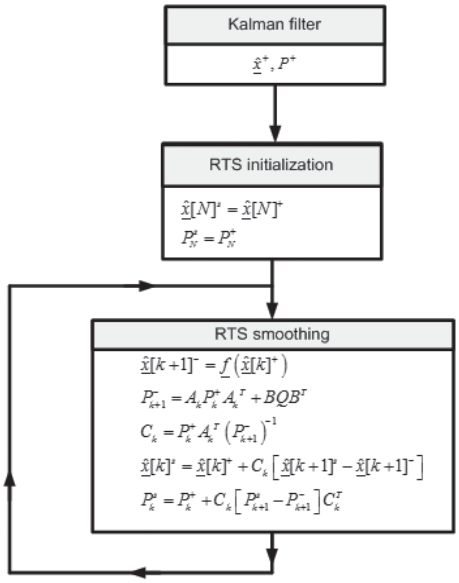

Figure 8. RTS smoother block diagram.

5 SIMULATION RESULTS

A. IMU Modeling and validation

Time rates of changes of IMU gimbals angles and time derivative of IMU velocity vector have been derived in previous sections. By solving theses differential equations using Runge-Kutta integration algorithm, IMU gimbals angles and velocities can be obtained.

Supposing that all IMU errors are zeros, the presented mathematical model could be compared with the perfect IMU model developed in SimMechanics.

Calibration process can be done in the any arbitrary test location, but albeit the longitude of the test position should be known. In the simulation the longitude of test position is considered as L=35.69° (The Tehran longitude).

Figure 9 illustrates IMU gimbals angles and velocity simulation results for IMU at in test location case.

Figure 10 illustrates perfect IMU gimbals angles and velocity simulation results for IMU at test location case by SimMechanics. Discontinuity in θ_x returns to MATLAB round process in[-180°,180°] range. These two figures show that the validity of the modeling.

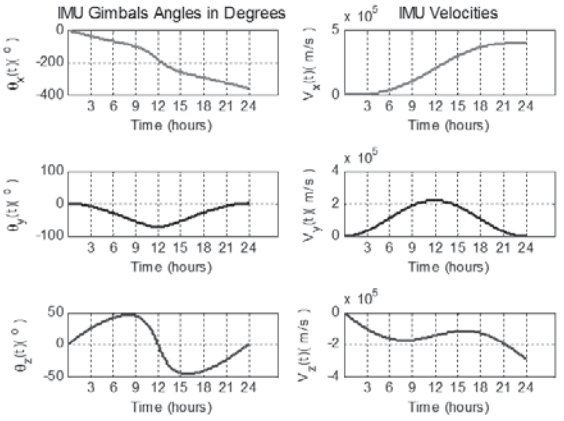

Figure 9. IMU output at test location (presented modeling).

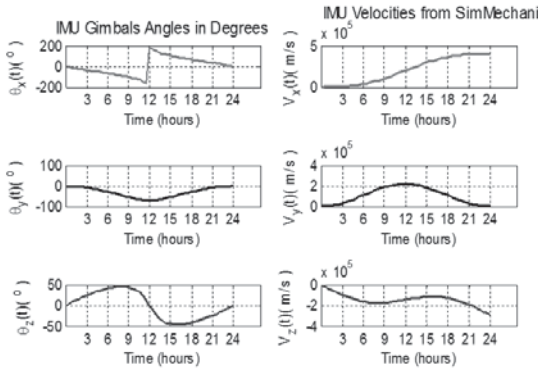

Figure 10. IMU model validation at test location (SimMechanics)

B. IMU Calibration

Assume that we select a proper sample rate and data saving time, an important question will arise: "how many attitudes should be selected for the specific sequence in the calibration process?". The answer to this question is not obvious question, but we can say that IMU parameters number to be calibrated affects the attitudes total number in a common sensegeneral wasy. As a result, selecting IMU calibration attitudes should be done by trial-and-error process until we reach to a confident sequence.

The finalized IMU platform test attitudes and corresponding gimbal angle rotations used in the implemented calibration process are illustrated in Figure 11.

Considering nine IMU platform attitudes with data sample rate of T=30 *sec* and attitude period of *attitude_time*=10 min, total measurement time during the calibration procedure is will be 90 minutes and total measurement count is will equal 189 samples×6 IMU outputs.

Figure 12 shows EKF estimation, forward-backward and RTS smoothers results for only platform x-axis accelerometer bias.

Measurement noise and process noise are both generated using MATLAB "randn" function; randn : returns a pseudorandom, scalar value drawn from a normal distribution with the mean of 0 and standard deviation of 1. To einsure the estimation results, more than few IMU data sets must be generated, then the calibration results for the IMU error parameters are averaged to get the final estimation results.

Considering the following noise standard deviation values:.

$$\begin{aligned}
&\sigma_{w_{\theta x}} = \sigma_{w_{\theta y}} = \sigma_{w_{\theta z}} = 6arc\ \min \\
&\sigma_{w_{V x}} = \sigma_{w_{V y}} = \sigma_{w_{V z}} = 0.2ms^{-1} \\
&\sigma_{V_{\theta x}} = \sigma_{V_{\theta y}} = \sigma_{V_{\theta z}} = 10arc\ \sec \\
&\sigma_{V_{V x}} = \sigma_{V_{V y}} = \sigma_{V_{V z}} = 0.1ms^{-1}
\end{aligned} \tag{31}$$

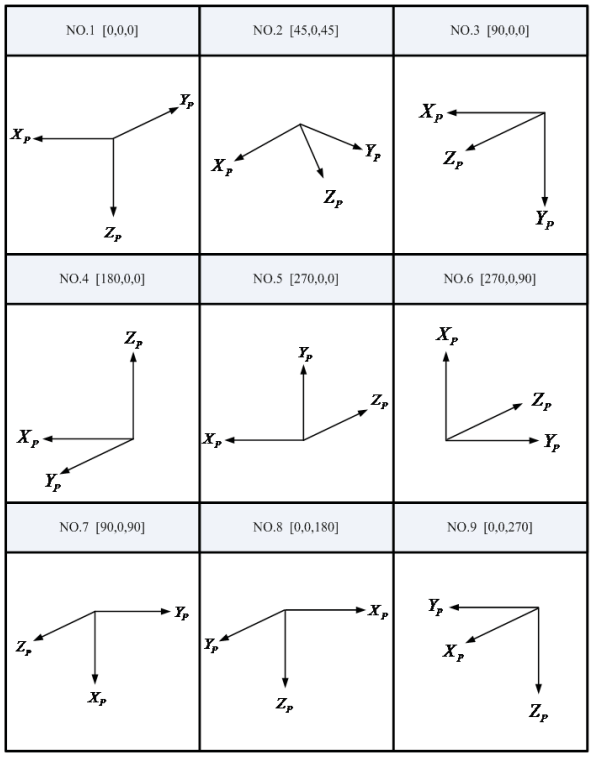

Figure 11. IMU platform test attitudes

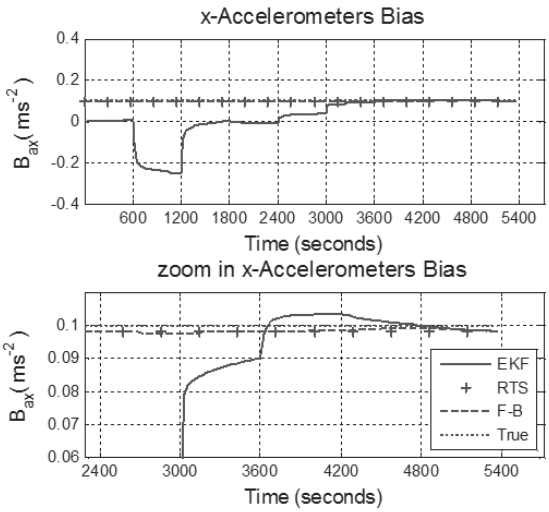

Figure 12. x accelerometer bias

Table 1 lists EKF, forward-backward, and RTS estimation results considering last EKF estimated value of the IMU error parameters and averaging the smoothed values for both forward-backward and RTS smoothers for 100 simulation runs.

As explained, for full calibration process the measurements of nine IMU platform different attitudes should be applied serially to the calibration algorithms.

Table 2 illustrates how the IMU calibration error sources become separable as a function of the cumulative number of platform test attitudes employed. As can be seen in this table, in the first four tests, no error sources could be estimated by the calibration algorithm. It means that up to this point, the measurements are not sufficiently enriched for estimating the error sources. By using the results of five other IMU platform different attitudes, the calibration algorithms could estimate some of the other error sources of each test.

Both sets of velocity and gimbals pickoffs angle measurements were assumed to be available. The x's indicates the earliest point at which the generated multiple sets of equations could be deterministically solved for a particular error source. All of the 15 IMU calibration errors can be determined after 9 platform attitudes times 6 specific equations per attitude or 54 equations are generated. Since only 15 equations should ideally be required, not all of the new equations generated are independent of previous ones.

6 CONCLUSION

In this paper, a mathematical model of 6-DOF gimballed IMU in space-stabilized mode is presented in detail. 15 error sources are incorporated in the developed model including gyroscopes drift vector, accelerometers bias vector, scale factor error vector, initial alignment imperfections and IMU case installation errors. Simulation results for three typical cases of non-rotating earth, equator case, and arbitrary location are presented. A validation technique using MATLAB SimMechanics tools is also presented and simulation results from both mathematical and SIMULINK models are compared to assure the correctness of mathematical model.

Assuming that all IMU error parameters are constants and using only system-level IMU outputs, simulation results show that employing 9 platform test attitudes is sufficient to separate all IMU calibration error sources, hence extended Kalman filter implementation brings out an accurate estimation values. Also, simulation results show that constant states are not smoothable and additional measurements are still helpful for refining an estimate of a constant state. However, there is no point in using smoothing for estimation of a constant state.

Glossary of variables

symbol	Description
${}^{i}_{n}C$	Navigation to inertial transformation matrix
$\theta_{x,y,z}$	Roll, pitch and yaw gimbals angles
D_g	Gyros drift vector
B_a	Accelerometers bias vector
ζ	Initial alignment error
η	IMU case installation error
${}^{p}\vec{\omega}_{p/i}$	Platform angular velocity relative to inertial coordinatized in platform frame
$\vec{f}_s$	Specific force vector
$\underline{w}$, $\underline{v}$	Gaussian, zero-mean, uncorrelated, white noises
$\mathrm{I_k}$	A (k×k) identity matrix
$\mathrm{P}^{+}_{\mathrm{k}}$	A priori covariance matrix
$\mathrm{P}^{-}_{\mathrm{k}}$	A posteriori covariance matrix
$\underline{\hat{x}}^{+}_{k}$	A posteriori state estimate
$\underline{\hat{x}}^{-}_{k}$	A priori state estimate
$\sigma_{w_{\theta_x}}$	θ_x system noise standard deviation
$\sigma_{v_{\theta_x}}$	θ_x measurement noise standard deviation
$\underline{\hat{x}}_f$	Forward state estimate
$\underline{\hat{x}}_b$	Backward state estimate
P_f	Forward covariance matrix
P_b	Backward covariance matrix
$\underline{\hat{x}}^{s}$	RTS smoother state estimation
P^{s}	RTS smoother covariance matrix

Table 1. IMU error calibration results for 100 simulation runs

symbol	True value		EKF		Forward-Backward		RTS	
			Estimated value	Estimation error%	Estimated value	Estimation error%	Estimated value	Estimation error%
B_{ax}	ms^{-2}	0.1	0.0981	1.90	0.0981	1.90	0.0981	1.90
B_{ay}		-0.2	-0.2043	2.15	-0.2031	1.55	-0.2043	2.15
B_{az}		0.3	0.2848	5.07	0.2847	5.10	0.2848	5.07
D_{gx}	°/hour	-0.4	-0.4034	0.85	-0.4032	0.80	-0.4034	0.85
D_{gy}		0.5	0.4868	2.64	0.4845	3.10	0.4868	2.64
D_{gz}		0.6	0.5994	0.10	0.6025	0.42	0.5994	0.10
dK_x	%	4	4.0331	0.83	4.0271	0.68	4.0331	0.83
dK_y		5	5.0649	1.30	5.0617	1.23	5.0649	1.30
dK_z		6	6.2234	3.72	6.2062	3.44	6.2234	3.72
ζ_x	arcmin	-5	-4.8930	2.14	-4.9429	1.14	-4.8930	2.14
ζ_y		3	3.0479	1.60	3.0332	1.11	3.0479	1.60
ζ_z		5	4.9706	0.59	4.9757	0.49	4.9706	0.59
η_x	arcmin	-5	-5.0236	0.47	-5.0254	0.51	-5.0236	0.47
η_y		2	1.8977	5.12	1.9463	2.69	1.8977	5.12
η_z		5	4.9270	1.46	4.9499	1.00	4.9270	1.46

Table 2. separation of IMU calibration parameters

Attitude	B_{ax}	B_{ay}	B_{az}	D_{gx}	D_{gy}	D_{gz}	dK_x	dK_y	dK_z	ζ_x	ζ_y	ζ_z	η_x	η_y	η_z
1															
2															
3															
4															
5		x						x				x			
6	x						x				x			x	
7					x								x		x
8				x		x				x					
9			x						x						

References

1. Jekeli C., Inertial Navigation System Geodetic, Walter de Gruyter GmbH & Co. KG, 2001.
2. Britting K.R., Inertial Navigation Systems Analysis, John Wiley & Sons, 1971.
3. Kitzerow R.A., Design, Development, Analysis, and Laboratory Test Results of a KALMAN Filter System-Level IMU Calibration Technique, *Technical Report AFAL-TR*-77-75, June 1977.
4. Syed Z., Aggarwal P., Niu X., Goodall C. and El-Sheimy N., A New Multi-Position Calibration Method for MEMS Inertial Navigation Systems, *Measurement Sience and Technology*, 18, 1897-1907, 2007.
5. Aggarwal P., Syed Z., Niu X. and El-Sheimy N., A Standard Testing and Calibration for Low Cost MEMS Inertial Sensors and Units, *Journal of Navigation*, 611, 323-336, 2008.
6. Shin E.H. and El-Sheimy N., A New Calibration

Method for Strapdown Inertial Navigation Systems, Z. Vermess, 127-10, 2002.

7. Fu L., Zhu Y., Wang L. and Wang X., A D-optimal Multi-position Calibration Method for Dynamically Tuned Gyroscopes, ELSEVIER, 2010.

8. Wang X. and Shen G., A Fast and Accurate Initial Alignment Method for Strapdown Inertial Navigation System on Stationary Base, *Journal of Control Theory and Applications*, vol. 3, no. 2, pp. 145-149, May 2005.

9. Wang X., Fast Alignment and Calibration Algorithms for Inertial Navigation System, *Aerospace science and technology*, vol. 13, no. 4-5, pp. 204-209, June-July 2009.

10. Hu C.H, Zheng J.F, Li J and Luo G.C, Rapid Self-Calibration for Small Gesture Inertial Platform before Launch, *Journal of Chinese Inertial Technology*, vol.3, 2007.

11. Yang L., Rapid Auto-Calibration for the Errors of Inertial Platform, *Journal of Chinese Inertial Technology*, vol.4, 2000.

12. Shin Y.J. and Kim C.J., Fast Calibration Technique for a Gimballed Inertial Navigation System, ICAS2002 CONGRESS, 2002.

13. Panahandeh G., Skog I. and Jansson M., Calibration of the Accelerometer Triad of an Inertial Measurement Unit, *Maximum Likelihood Estimation and Cramér-Rao Bound, IPIN International Conference*, 15-17 September 2010, Zurich, Switzerland, 2010.

14. Ozgoli S. and Arvan M.R., Modeling and Simulation of Moving system, Ya Mahdi Publication, Tehran, Iran, 2010, (in Persian).

15. Simon D., Optimal State Estimation: Kalman, .A, and Nonlinear Approaches, John Wiley & Sons, 2006.

16. Khodadadi H., Jahed Motlagh M.R. and Gorji M., Robust Control and Modeling a 2-DOF Inertial Stabilized Platform, *International Conference on Electrical, Control and Computer Engineering Pahang, Malaysia*, June 21-22, 2011.